The rigid core and flexible surface of amyloid fibrils probed by Magic-Angle Spinning NMR of aromatic residues

Lea Marie Becker, Mélanie Berbon, Alicia Vallet, Axelle Grelard, Estelle Morvan, Benjamin Bardiaux, Roman Lichtenecker, Matthias Ernst, Antoine Loquet, Paul Schanda

The Rigid Core and Flexible Surface of Amyloid Fibrils Probed by Magic-Angle-Spinning NMR Spectroscopy of Aromatic Residues

Lea Marie Becker[a], Mélanie Berbon[b] Alicia Vallet,[c] Axelle Grelard,[b] Estelle Morvan,[d] Benjamin Bardiaux,[e] Roman Lichtenecker,[f] Matthias Ernst[g], Antoine Loquet[b] and Paul Schanda*[a]

Dedicated to Robert Konrat, on the occasion of his 60th birthday.

Aromatic side chains are important reporters of the plasticity of proteins, and often form important contacts in protein–protein interactions. We studied aromatic residues in the two structurally homologous cross-β amyloid fibrils HET-s, and HELLF by employing a specific isotope-labeling approach and magic-angle-spinning NMR. The dynamic behavior of the aromatic residues Phe and Tyr indicates that the hydrophobic amyloid core is rigid, without any sign of "breathing motions" over hundreds of milliseconds at least. Aromatic residues exposed at the fibril surface have a rigid ring axis but undergo ring flips on a variety of time scales from nanoseconds to microseconds. Our approach provides direct insight into hydrophobic-core motions, enabling a better evaluation of the conformational heterogeneity generated from an NMR structural ensemble of such amyloid cross-β architecture.

[a] L. M. Becker, P. Schanda*
Institute of Science and Technology Austria, Am Campus 1, 3400 Klosterneuburg, Austria
E-mail: paul.schanda@ista.ac.at

[b] A. Grelard, M. Berbon, A. Loquet
Univ. Bordeaux, CNRS, Bordeaux INP, CBMN, UMR 5248, IECB, Pessac, France

[c] A. Vallet
Institut de Biologie Structurale, 41, avenue des martyrs, Grenoble, France

[d] E. Morvan
Institut Européen de Chimie et Biologie UAR3033 CNRS, University of Bordeaux, INSERM US01, Pessac, France

[e] B. Bardiaux
Bacterial Transmembrane Systems Unit, Institut Pasteur, Université Paris Cité, CNRS UMR 3528, 75015 Paris, France.
Structural Bioinformatics Unit, Institut Pasteur, Université Paris Cité, CNRS UMR 3528, 75015 Paris, France.

[f] R. Lichtenecker
Institute of Organic Chemistry, University of Vienna, Währinger Str. 38, 1090 Vienna, Austria

[g] M. Ernst
Physical Chemistry, ETH Zürich, Vladimir Prelog Weg 2, CH-8093 Zürich, Switzerland

Introduction

Aromatic side chains play important roles for protein stability and function: located at active sites or entry gates of enzymes or membrane channels[1], and over-represented at protein–protein interfaces[2], aromatic groups are directly involved in binding or enzymatic turnover. Moreover, they stabilize protein folds by forming π–π[3,4], CH–π[5,6], or cation–π[7] interactions and promote self-assembly of amyloid proteins[8]. The bulky nature of phenylalanines (Phe), tyrosines (Tyr), and tryptophans (Trp) brings an interesting aspect to their dynamics: flips of the ring by 180°, which lead to the inter-conversion of indistinguishable states (for Phe and Tyr), are accompanied by significant energy barriers. Ring flips were already observed in solution by nuclear magnetic resonance (NMR) spectroscopy in the 1970s[9–11]. They are thought to require "breathing motions", i.e. transient excursions of the protein to conformationally excited states that create the void volume required for the flip to occur. Consequently, studying ring-flip rates as a function of temperature[12,13] or pressure[14,15] can shed light on activation energies of the underlying structural excursions. In a recent study, ring-flips of a Tyr in an SH3 domain have been studied; in addition to ring flips, an excited state, ascribed to "breathing motions" has been structurally characterized.[16] Continuous development of solution-NMR methodology, in particular relaxation-dispersion methods[17–19], and specific isotope labeling[20,21], has allowed the study of ring dynamics at an increasing level of detail in soluble proteins of moderate size[22]. Large protein complexes and insoluble proteins can instead be studied by magic-angle-spinning (MAS) NMR. As overall tumbling is absent, the study of protein dynamics by MAS NMR focuses on internal motion through observation of the partial averaging of anisotropic interactions (dipolar couplings, chemical-shift anisotropy) and through spin relaxation[23]. Recent studies have probed aromatic ring dynamics in small crystalline proteins[24–26], membrane proteins in lipid bilayers[27], as well as motions in large protein assemblies, including experiments at temperatures down to 100 K[28].

Amyloid fibrils assemble into a cross-β architecture from basic building blocks to quasi-infinitely long β-sheets with a rigid, water-excluding core[29,30]. Dynamics of amyloid fibrils are much less studied than those of globular proteins, and it is not clear whether the core of such fibrils undergoes "breathing motions" or if those are suppressed by the collective nature of densely packed β-sheets. Backbone dynamics of HET-s have been studied by MAS NMR[31], and have

pointed to a largely rigid core, but such data can hardly capture rare events such as ring flips and breathing motion. Aromatic residues at the *surface* of amyloids formed by the HET-s(218-289) protein have been shown to be important for fibril propagation,[32] suggesting that aromatic side chains may be important for forming inter-subunit contacts. This raises the question of how flexible their surface-exposed residues are.

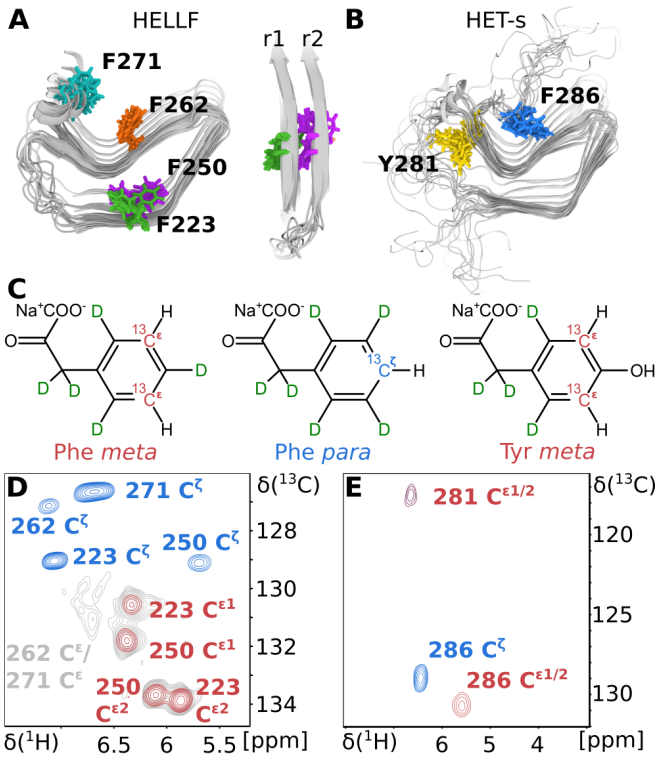

Figure 1. MAS NMR of aromatic side chains in HELLF (A, D) and HET-s (B, E) amyloids. (A, B) Structural ensemble (ten lowest-energy structures of HELLF, PDB: 6EKA,[33], and HET-s, PDB: 2KJ3,[34]) The right panel in (A) shows the view on the side of HELLF with the repeats r1 and r2. Only one subunit of the quasi-infinite fiber is shown. (C) α-Ketoacid precursors[21] used herein, yielding either an isolated ^{1}H–^{13}C pair in the ζ-position of Phe (middle) or two ^{1}H–^{13}C pairs in the ε-positions (left, right). (D, E) ^{1}H-^{13}C dipolar-coupling-based correlation spectra of *meta*-Phe (red) and *para*-Phe (blue) labeled HELLF (D) and *meta*-Phe (red), *para*-Phe (blue) and *meta*-Tyr (red) labeled HET-s (E) with resonance assignments (55 kHz MAS; 14.1 T field strength; see supplementary information for details). The grey spectrum in (D) is the same as the red one but plotted with lower contourlevels, showing the broadened peak which presumably belongs to *meta*-CH of Phe262 or Phe271.

Here we investigate the dynamics of the aromatic residues Phe and Tyr in a pair of structurally homologous and functional fungal amyloid fibrils, HET-s(218-289) and HELLF(209-277) (called HET-s and HELLF in the following). The three-dimensional structures of the fibrils, obtained from MAS NMR[33,34], show a β-solenoid core consisting of two repeats (r1 and r2) approximately 30 residues long that form two layers of β-strands arranged to a triangular core. The flanking regions and the loop connecting the two layers are unstructured, highly mobile, and not visible by cross-polarization ^{13}C MAS NMR[35]. In the NMR structures, the aromatic residues adopt a range of conformations (Fig. 1A, B). In HELLF, two Phe residues are located in the rigid amyloid core: Phe223 and Phe250 belong respectively to the r1 and r2 repeats and are located above each other, pointing toward the hydrophobic core. The exact nature of their interaction remained elusive in the NMR structure ensemble and the two aromatic rings adopt various χ1 and χ2 angles (Fig. 1A). This either suggests significant flexibility of the side chains within the hydrophobic core or an insufficiently well-defined structure, possibly due to the lack of distance restraints. While one may argue that the exact location of these side chains is a detail, it bears important implications: whether or not these aromatic rings adopt multiple conformations directly reports on the plasticity of the hydrophobic core and, thus, more generally on breathing motions in amyloid fibrils. Two other aromatic residues are Phe262, involved in r2 but with its aromatic ring pointing outside the amyloid core, and Phe271, not involved in the amyloid core but in the C-terminal flanking region. HET-s has a tyrosine and a phenylalanine residue (Tyr281, Phe286). Tyr281, located at the very end of the last β-strand of r2, has been shown to have increased $^{13}C^{\alpha}$ $R_{1\rho}$ relaxation, and its side chain points toward the putative C-terminal semi-hydrophobic pocket[32] while Phe286 is not involved in the amyloid core and is located in the C-terminal flanking region.

Results and Discussion

To selectively observe aromatic residues, we have used a specific isotope labeling approach (Fig. 1C) which consists of introducing isolated ^{1}H-^{13}C pairs at either the ε positions of Phe or Tyr or the ζ position in Phe, in an otherwise deuterated and natural-abundance carbon background[21]. This approach allows for sensitive ^{1}H detection at high resolution, and the simplicity of the spin system reduces additional spin-relaxation mechanisms and allows to interpret relaxation data in a straightforward manner. The spin pair dynamics at the ζ position (referred to as *para*-CH henceforth) reports exclusively on ring-axis motion but is insensitive to ring flips, while the ε spin pairs (*meta*-CH) get reoriented by ring flips and are thus sensitive reporters of flips. In the case of no flips or flips on timescales longer than tens of milliseconds (ms), one would expect two sets of *meta*-CH peaks corresponding to the two ε sites being in different environments. Very rapid ring flips would lead to a single averaged peak, while flips occurring on a time scale from hundreds of ns to ca. one ms result in very fast spin relaxation that strongly broadens resonance peaks (Fig. S2). Figures 1D and 1E show the high-resolution ^{1}H-detected MAS NMR spectra of HELLF and HET-s, respectively, labeled with either *meta*-CH (red) or *para*-CH (blue) spin pairs in otherwise deuterated samples in H_2O-based buffer. We have used three-dimensional through-space ^{1}H-^{1}H-(^{13}C/^{15}N) spectra (time-shared ^{13}C/^{15}N dimension) to assign all observed cross-peaks via spatial proximity to backbone amides (Fig. S3 and S4). For all *para*-CH pairs, we detect a single cross-peak, as expected. The case of the *meta*-CH spectra, however, reveals an interesting variety of behaviors: (i) Tyr281 and Phe286 located at the C-terminus of HET-s (last strand and adjacent terminus) show a single cross-peak pointing to rapid ring flips (Fig. 1E). (ii) Phe223 and Phe250 in the core of HELLF, in contrast, show separate cross peaks for the $^{1}H^{\varepsilon 1}$–$^{13}C^{\varepsilon 1}$ and $^{1}H^{\varepsilon 2}$–$^{13}C^{\varepsilon 2}$ sites, revealing the absence of fast ring flips (Fig. 1D). (iii) The signals of Phe262 and Phe271 could not be unambiguously identified. A broad resonance, detected in several indepen-

dent samples at ca. 6.6 ppm/131 ppm, is tentatively ascribed to the *meta*-CH sites of one or both of these Phe rings (Fig. 1D, grey spectrum). In any case, it is obvious that the *meta*-CH signals of Phe262 and Phe271 are heavily broadened, while their *para*-CH resonances yield sharp lines; these findings strongly suggest that Phe262 and Phe271 undergo ring flips on a time scale that leads to maximum broadening (hundreds of ns to hundreds of µs; Fig. S2, discussed below; Fig. S8).

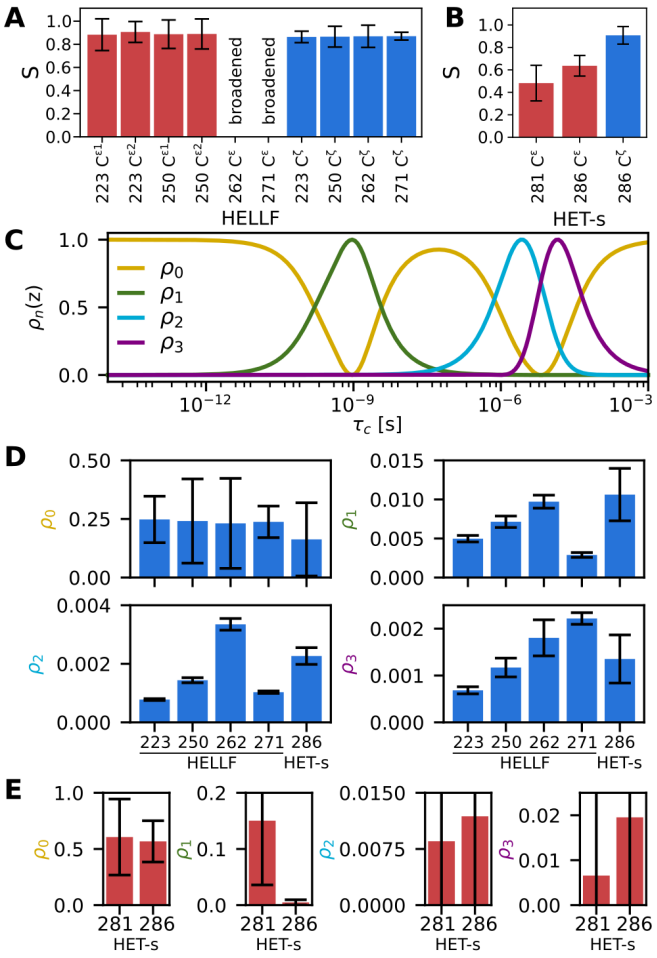

Figure 2. Dynamics measurements from ^{13}C-^{1}H dipolar order parameters and ^{13}C relaxation data of *para*-CH (blue) and *meta*-CH (red) sites in Phe and Tyr. (A, B) REDOR-derived dipolar order parameters. (C-E) Fits with the DETECTORS approach. (C) Detector sensitivities showing the time scales on which each detector reports, τ_c is the correlation time of the motion. Note that ρ_0, given by the difference between ρ_1–ρ_3 and the dipolar order parameter, primarily reflects sub-µs motions, as dipolar couplings report on motion only up to ca. 10 µs. (D, E) Site-specific responses to the detectors that reflect amplitudes of motion.

We have obtained quantitative information about ring-axis motion and ring flips via ^{1}H–^{13}C dipolar-coupling and ^{13}C spin-relaxation measurements [23]. Dipolar-coupling tensors report on the reorientational averaging of the H-C bond on time scales shorter than tens of µs, which is conveniently expressed as the order parameter S ($S \in [0;1]$ where S=1 indicates a rigid bond). These data reveal that the ring axes of all Phes in HELLF and HET-s undergo only low-amplitude motions (S ca. 0.9; Fig. 2A and B; Tab. S2 and S3). Relaxation measurements are also sensitive to the time scales of motion, in addition to amplitudes. We have measured ^{13}C longitudinal relaxation (R_1) as well as rotating-frame ^{13}C relaxation ($R_{1\rho}$) to gain insights into the time scales of motions (Fig. S5, S6, S7; Tab. S4 and S5). R_1 is mostly sensitive to motion from hundreds of ps to ten ns, while $R_{1\rho}$ senses motions on hundreds-of-ns to hundreds-of-µs time scales depending on the strengths of the applied spin-lock radio-frequency (RF) field (ν_{RF}). $R_{1\rho}$ rate constants at variable spin-lock radio-frequency (RF) field strengths [36,37] probe ns-ms motions; in particular NEar-rotary Resonance Relaxation-Dispersion (NERRD) [38], specifically reveal µs–ms dynamics.

We have used the DETECTORS approach [39] for a joint analysis of the relaxation data and dipolar order parameters (Fig. 2C-E). This approach reports the amplitudes of motion occurring in various time windows characterized by so-called responses (ρ_0, ρ_1, ρ_2, ρ_3; Fig. 2C), taking into account that different relaxation parameters are differently sensitive to different time scales. ρ_1, ρ_2 and ρ_3 are derived from the relaxation data, while ρ_0 reflects the residual amplitude, i.e. the difference to the dipolar-coupling derived squared order parameter S^2. Molecular dynamics results have suggested that for the backbone, ρ_0 motions mostly correspond to fast motions (sub-µs) [31].

The *para*-CH sites, which sense ring-axis motions, show mostly fast motions: the majority of the motional amplitude is covered by the ρ_0 and (less) by ρ_1; it seems indeed plausible that the small-amplitude librational motions occur on short time scales (ps-ns). DETECTORS analysis of the *meta*-CH sites of Tyr281 reveals ring flips occurring predominantly on short time scales (mostly ρ_0 and ρ_1 - ns); as Tyr281 points towards a loose cavity formed by a highly flexible [31] loop, this result appears plausible. Phe286 (HET-s) differs from Tyr281 as it shows essentially no ρ_1 (ns) response and more contributions from slower motions (ρ_2, ρ_3). Although Phe286 points towards the outside of the fibril, we ascribe the retardation of its ring flips to contacts with the surface, with a possible candidate for a CH-π interaction with H$^{\beta}$ of Gln240. This observation is in line with the reduced prion activity of the mutants F286A and Q240A [32], attributed to their close proximity and their putative role in structurally maintaining the C-terminal pocket region. No sharp correlation peaks are observed for Phe262 and Phe271 (HELLF) and only a broad peak is tentatively assigned to these sites. Such broadening is presumably due to motions on time scales of hundreds of ns to a ms (Fig. S2). Temperature-dependent spectra show that the intensity of this broad peak increases with temperature (Fig. S8), indicating that accelerating the motions leads to lower relaxation rate constants, and, thus, that the motion occurs on the sub-µs time scale. Of note, the ring axes of Phe262 and Phe271 do not undergo extensive µs motions as their order parameters are high (Fig. 2A). A modest NERRD effect suggests the presence of small-amplitude µs motion (Fig. S7E). Taken together, the surface-exposed side chains of F262 and F271 appear to undergo ns–µs dynamics.

To investigate whether or not the amyloid core allows for breathing motions, we addressed whether the two Phe residues in the core of HELLF, Phe223 and Phe250, undergo ring flips. The fact that individual cross-peaks are observed for the ^{1}H$^{\varepsilon1}$–^{13}C$^{\varepsilon1}$ and ^{1}H$^{\varepsilon2}$–^{13}C$^{\varepsilon2}$ sites shows that there are either no or very slow flips (at least tens-hundreds of ms). We performed longitudinal exchange experiments, in which the ^{13}C indirect chemical-shift evolution period and

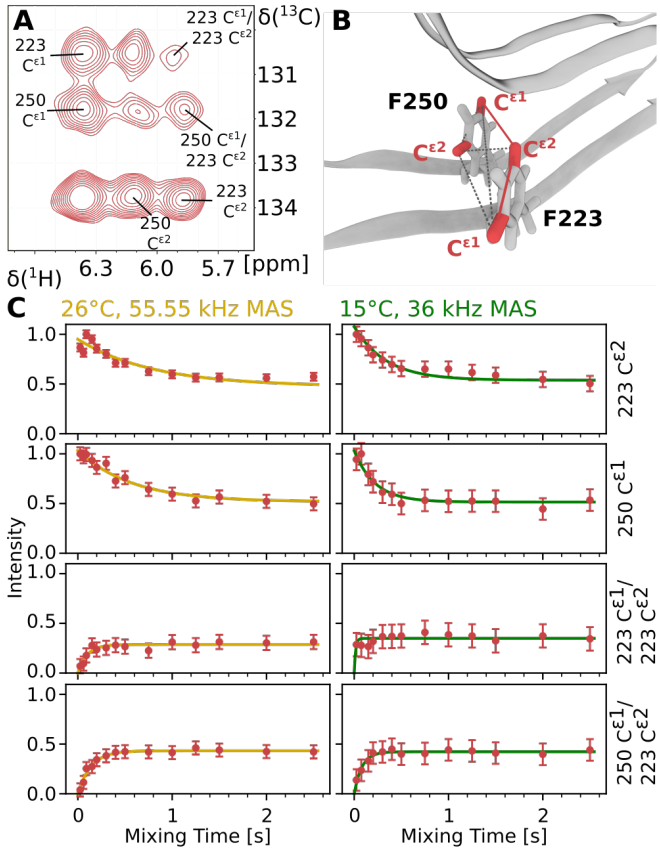

Figure 3. ^{13}C longitudinal mixing (EXchange SpectroscopY/spin diffusion) experiment of the *meta*-CH sites of Phe223 and Phe250 (HELLF). (A) Exchange spectrum with a mixing time of 2500 ms. (B) Location of the two aromatic rings in one of the structures of PDB 6EKA,[33] (C). Time traces, i.e., the evolution of peak intensities as a function of the longitudinal mixing time.

the ^{1}H acquisition are separated by a C_z mixing period. During this period two processes may occur: (i) in the case of ring flips, the ^{13}C frequency of one ε site is linked to the ^{1}H frequency of the other ε site; (ii) in the absence of ring flips, the two ^{13}C nuclei in the ring exchange their magnetization by (proton-driven) spin diffusion. The outcome would be identical, i.e. $^{13}C^{\varepsilon1}$-$^{1}H^{\varepsilon2}$ and $^{13}C^{\varepsilon2}$-$^{1}H^{\varepsilon1}$ cross peaks would be observed. A series of measurements with increasing mixing time shows indeed cross-peaks (Fig. 3A), which build up with a time constant of ca. 100 ms (Fig. 3B,C and S9; Tab. S6). The two processes, ring flips and spin diffusion, can be disentangled because the former is expected to be temperature-dependent but not MAS-frequency dependent, while spin diffusion is strongly MAS-frequency dependent[40]. Experiments at lower MAS frequency show a strongly accelerated buildup of the cross-peaks (Fig. 3C right panel), unambiguously demonstrating that the observed cross-peaks are due to spin diffusion, and not to ring flips. Moreover, cross-peaks between sites of Phe223 and Phe250 have a similar buildup rate constant, and these signals can only be due to magnetization exchange, not ring flips. In support of this view, spin dynamics simulations show transfer on the tens of ms timescale (Fig. S10). These data allow us to conclude that the Phe rings (Phe223 and Phe250) in the hydrophobic core do not undergo flips on time scales of at least hundreds of milliseconds, demonstrating the absence of "breathing motions" of the fibril over at least this time scale.

Having shown that the aromatic rings in the core of HELLF are rigid – contrasting the previously determined structural ensemble – we carried out new structure calculations: we supplemented the previously used distance restraints[33] by 9 additional restraints, determined in the present study, that involve F223 and F250 (details can be found in the caption of Fig. S11). The resulting NMR conformer ensemble (Fig. S11) shows a better-defined, stacked position of F223 and F250, thus reconciling the dynamics data with the structural ensemble.

Conclusion

In conclusion, we have demonstrated that specific ^{1}H/^{13}C/^{2}H labeling with sensitive ^{1}H MAS NMR provides detailed insight into ring dynamics in amyloid fibrils. We find a wide range of dynamic scenarios, with ring flips occurring on time scales of a few nanoseconds to (at least) many hundreds of milliseconds. Interestingly, Phe rings on the outside of the fibril (Phe262, Phe271, Phe286) all undergo slow flips (hundreds of ns to µs). This is in contrast to e.g. Phe rings at the surface of the globular microcrystalline ubiquitin (ca. 10 ns)[41], and suggests that aromatic ring flips might be slowed down by possible transient side chain-side chain contacts taking place at the fibril surface, possibly through CH-π interactions. Alternatively or additionally, the rings that appear exposed in the HET-s and HELLF structures might be in contact with neighboring protofibrils. Indeed, a low-resolution electron-microscopy structure[42] of HET-s assembled at pH 3 revealed close lateral contacts between fibrils. However, the fibrils used in the present study, obtained at neutral pH differ significantly from those obtained under acidic conditions[43]. Previous NMR data suggest that there are no stable, defined inter-protofilament contacts in MAS NMR studies of HELLF[33] and HETs[34] and solvent-accessibility data by NMR furthermore suggested that the protofilament is surrounded by water[29]. Mass-per-length measurements confirm that both, HET-s and HELLF, exist as a single filament under the conditions used for NMR spectroscopy[33,44]. Importantly, our results imply that the structural heterogeneity observed at the level of aromatic side chains in the MAS NMR structure ensemble of amyloid fibrils (here: F223 and F250, which are disordered in the deposited MAS NMR structure) does not reflect the actual dynamics. This study highlights the capacity of MAS NMR to combine distance restraint collection and specific dynamics measurement to provide a conformational picture of the cross-β amyloid architecture.

Acknowledgements

We thank Albert A. Smith (Leipzig) for insightful discussions. This work was supported by funding from the European Research Council (StG-2012-311318 to P.S.) and used the platforms of the Grenoble Instruct-ERIC center (ISBG; UMS 3518 CNRS-CEA-UJF- EMBL) within the Grenoble Partnership for Structural Biology (PSB) and facilities and expertise of the Biophysical and Structural Chemistry platform (BPCS) at IECB, CNRS UAR3033, INSERM US001 and Bordeaux University.

Conflict of Interest

The authors do not have conflicts of interest.

Keywords: aromatic side chains • isotopic labeling • protein dynamics • ring flips • spin relaxation

References

[1] H.-X. Zhou, J. A. McCammon, *Trends Biochem. Sci.* **2010**, *35*, 179.
[2] E. Lanzarotti, L. A. Defelipe, M. A. Marti, A. G. Turjanski, *J. Cheminformatics* **2020**, *12*.
[3] S. Burley, G. A. Petsko, *Science* **1985**, *229*, 23.
[4] G. B. McGaughey, M. Gagné, A. K. Rappé, *J. Biol. Chem.* **1998**, *273*, 15458.
[5] T. Steiner, G. Koellner, *J. Mol. Biol.* **2001**, *305*, 535.
[6] M. F. Perutz, *Philos. Trans. R. Soc. A* **1993**, *345*, 105.
[7] J. C. Ma, D. A. Dougherty, *Chem. Rev.* **1997**, *97*, 1303.
[8] E. Gazit, *FASEB J* **2002**, *16*, 77.
[9] I. D. Campbell, C. M. Dobson, R. J. P. Williams, *Proc. R. Soc. B.* **1975**, *189*, 503.
[10] G. Wagner, A. DeMarco, K. Wüthrich, *Biophys. Struct. Mech.* **1976**, *2*, 139.
[11] K. Wuthrich, G. Wagner, *Trends Biochem. Sci.* **1978**, *3*, 227.
[12] J. J. Skalicky, J. L. Mills, S. Sharma, T. Szyperski, *J. Am. Chem. Soc.* **2001**, *123*, 388.
[13] M. Hattori, H. Li, H. Yamada, K. Akasaka, W. Hengstenberg, W. Gronwald, H. R. Kalbitzer, *Prot. Sci.* **2004**, *13*, 3104.
[14] M. Dreydoppel, B. Dorn, K. Modig, M. Akke, U. Weininger, *JACS Au* **2021**, *1*, 833.
[15] G. Wagner, *FEBS Lett.* **1980**, *112*, 280.
[16] L. Mariño Pérez, F. S. Ielasi, L. M. Bessa, D. Maurin, J. Kragelj, M. Blackledge, N. Salvi, G. Bouvignies, A. Palencia, M. R. Jensen, *Nature* **2022**, *602*, 695.
[17] U. Weininger, M. Respondek, C. Low, M. Akke, *J. Phys. Chem. B* **2013**, *117*, 9241.
[18] U. Weininger, K. Modig, M. Akke, *Biochemistry* **2014**, *53*, 4519.
[19] H. N. Raum, M. Dreydoppel, U. Weininger, *J. Biomol. NMR* **2018**, *72*, 105.
[20] V. Kasinath, K. G. Valentine, A. J. Wand, *J. Am. Chem. Soc.* **2013**, *135*, 9560.
[21] R. J. Lichtenecker, K. Weinhäupl, W. Schmid, R. Konrat, *J. Biomol. NMR* **2013**, *57*, 327.
[22] M. Akke, U. Weininger, *J. Phys. Chem. B* **2023**, *127*, 591.
[23] P. Schanda, M. Ernst, *Prog. Nucl. Magn. Reson. Spectrosc.* **2016**, *96*, 1.
[24] M. J. Potrzebowski, P. Paluch, T. Pawlak, A. Jeziorna, J. Trébosc, G. Hou, A. Vega, J.-P. Amoureux, M. Dracinsky, T. Polenova, *Phys. Chem. Chem. Phys.* **2015**, *17*, 28789.
[25] C. Gall, T. Cross, J. DiVerdi, S. Opella, *Proc. Natl. Acad. Sci.* **1982**, *79*, 101.
[26] L. Vugmeyster, D. Ostrovsky, T. Villafranca, J. Sharp, W. Xu, A. S. Lipton, G. L. Hoatson, R. L. Vold, *J. Phys. Chem. B* **2015**, *119*, 14892.
[27] F. Hu, W. Luo, M. Hong, *Science* **2010**, *330*, 505.
[28] D. F. Gauto, P. Macek, A. Barducci, H. Fraga, A. Hessel, T. Terauchi, D. Gajan, Y. Miyanoiri, J. Boisbouvier, R. Lichtenecker, et al., *J. Am. Chem. Soc.* **2019**, *141*, 11183.
[29] H. Van Melckebeke, P. Schanda, J. Gath, C. Wasmer, R. Verel, A. Lange, B. H. Meier, A. Böckmann, *J. Mol. Biol.* **2011**, *405*, 765.
[30] I. Kheterpal, A. Williams, C. Murphy, B. Bledsoe, R. Wetzel, *Biochemistry* **2001**, *40*, 11757.
[31] A. A. Smith, E. Testori, R. Cadalbert, B. H. Meier, M. Ernst, *J. Biomol. NMR* **2016**, *65*, 171.
[32] A. Daskalov, M. Gantner, M. A. Wälti, T. Schmidlin, C. N. Chi, C. Wasmer, A. Schütz, J. Ceschin, C. Clavé, S. Cescau, B. Meier, R. Riek, S. J. Saupe, *PLOS Pathogens* **2014**, *10*.
[33] A. Daskalov, D. Martinez, V. Coustou, N. El Mammeri, M. Berbon, L. B. Andreas, B. Bardiaux, J. Stanek, A. Noubhani, B. Kauffmann, et al., *Proc. Natl. Acad. Sci. USA* **2021**, *118*.
[34] H. Van Melckebeke, C. Wasmer, A. Lange, E. Ab, A. Loquet, A. Böckmann, B. H. Meier, *J. Am. Chem. Soc.* **2010**, *132*, 13765.
[35] A. B. Siemer, A. A. Arnold, C. Ritter, T. Westfeld, M. Ernst, R. Riek, B. H. Meier, *J. Am. Chem. Soc.* **2006**, *128*, 13224.
[36] R. Kurbanov, T. Zinkevich, A. Krushelnitsky, *J. Chem. Phys.* **2011**, *135*.
[37] J. R. Lewandowski, H. J. Sass, S. Grzesiek, M. Blackledge, L. Emsley, *J. Am. Chem. Soc.* **2011**, *133*, 16762.
[38] V. Kurauskas, S. A. Izmailov, O. N. Rogacheva, A. Hessel, I. Ayala, J. Woodhouse, A. Shilova, Y. Xue, T. Yuwen, N. Coquelle, et al., *Nat. Commun.* **2017**, *8*.
[39] A. A. Smith, M. Ernst, B. H. Meier, *J. Chem. Phys.* **2018**, *148*.
[40] A. Grommek, B. H. Meier, M. Ernst, *Chem. Phys. Lett.* **2006**, *427*, 404.
[41] D. F. Gauto, O. O. Lebedenko, L. M. Becker, I. Ayala, R. Lichtenecker, N. R. Skrynnikov, P. Schanda, *J. Struct. Biol. X* **2023**, *7*.
[42] N. Mizuno, U. Baxa, A. C. Steven, *Proc. Natl. Acad. Sci. USA* **2011**, *108*, 3252.
[43] R. Sabaté, U. Baxa, L. Benkemoun, N. S. de Groot, B. Coulary-Salin, M.-l. Maddelein, L. Malato, S. Ventura, A. C. Steven, S. J. Saupe, *J. Mol. Biol.* **2007**, *370*, 768.
[44] B. Chen, K. R. Thurber, F. Shewmaker, R. B. Wickner, R. Tycko, *Proc. Natl. Acad. Sci. USA* **2009**, *106*, 14339.

Entry for the Table of Contents

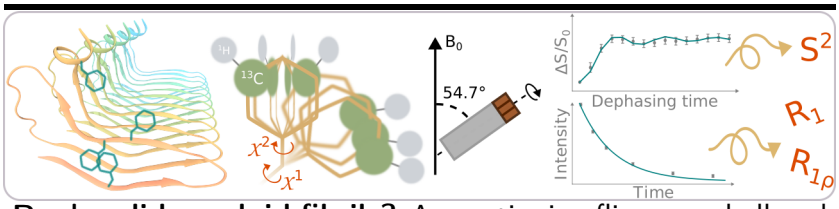

Rock-solid amyloid fibrils? Aromatic ring flips are a hallmark of "breathing motions" in proteins. But does the infinitely long β-sheet structure of amyloids allow for such motions? In their Article, Becker *et al.* apply specific isotope labeling and solid-state NMR to two amyloid fibrils to demonstrate that the motion of aromatic rings strongly differs between the core and the surface of the fibril.

Twitter: @LabSchanda